



HAL
open science

Raman confocal microscopy and biophysics multiparametric characterization of the skin barrier evolution with age

Aline Rigal-Dachaud, Rime Michael-Jubeli, Alex Nkengne, Arlette
Baillet-Guffroy, Armelle Bigouret, Ali Tfayli

► **To cite this version:**

Aline Rigal-Dachaud, Rime Michael-Jubeli, Alex Nkengne, Arlette Baillet-Guffroy, Armelle Bigouret, et al.. Raman confocal microscopy and biophysics multiparametric characterization of the skin barrier evolution with age. *Journal of Biophotonics*, 2021, 14 (9), pp.e202100107. 10.1002/jbio.202100107. hal-04528043

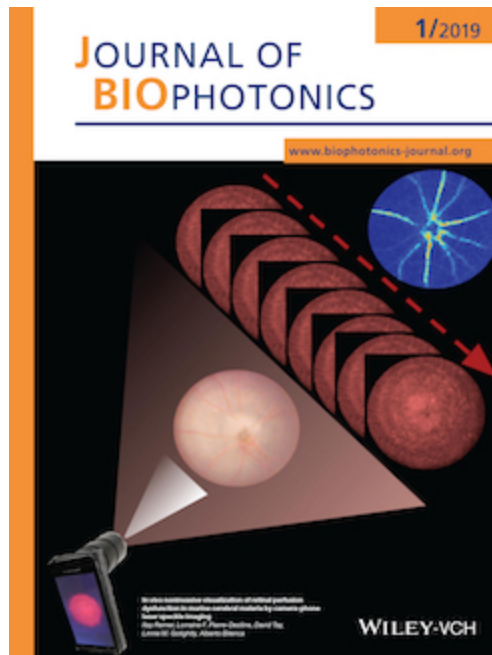
HAL Id: hal-04528043

<https://hal.science/hal-04528043>

Submitted on 3 Apr 2024

HAL is a multi-disciplinary open access archive for the deposit and dissemination of scientific research documents, whether they are published or not. The documents may come from teaching and research institutions in France or abroad, or from public or private research centers.

L'archive ouverte pluridisciplinaire **HAL**, est destinée au dépôt et à la diffusion de documents scientifiques de niveau recherche, publiés ou non, émanant des établissements d'enseignement et de recherche français ou étrangers, des laboratoires publics ou privés.



Raman Confocal Microscopy and biophysics multi-parametric characterization of the skin barrier evolution with age.

Journal:	<i>Journal of Biophotonics</i>
Manuscript ID	Draft
Wiley - Manuscript type:	Full Article
Date Submitted by the Author:	n/a
Complete List of Authors:	Rigal, Aline; Universite Paris-Saclay, Pharmacy Michael-Jubeli, Rime; Universite Paris-Saclay, Pharmacy Nkengne, Alex; Laboratoires Clarins SAS Baillet-Guffroy, Arlette; Universite Paris-Saclay, Pharmacy Bigouret, Armelle; Laboratoires Clarins SAS Tfayli, Ali ; Universite Paris-Saclay, Pharmacy
Keywords:	In vivo Raman spectroscopy, Skin aging, Biophysics parameters, Skin lipids

SCHOLARONE™
Manuscripts

1
2
3 **Titre: Raman Confocal Microscopy and biophysics multi-parametric characterization of the skin**
4 **barrier evolution with age**
5
6
7
8

9 Aline RIGAL¹, Rime MICHAEL-JUBELI¹, Alex NKENGNE², Arlette BAILLET-GUFFROY¹, Armelle BIGOURET²,
10 Ali TFAYLI^{1*}
11
12
13
14
15

16 ¹ “Lipides: Systèmes Analytiques et Biologiques” Lip(Sys)2 interdisciplinary unit, Faculty of Pharmacy,
17 University Paris-Saclay, Châtenay-Malabry 92290,
18
19

20 ² Clarins Laboratories, Pontoise 95300
21
22
23
24
25

26 **Abstract**
27

28 Skin aging is a multifactorial phenomenon that involves alterations at the molecular, cellular, and tissue
29 levels. Our aim was to carry out a multiparametric biophysical and Raman characterization of skin
30 barrier between individuals of different age groups (<24 and > 70 years old).
31
32

33 Our results showed a significant decrease of lipids to proteins ratio overall the thickness of the SC and
34 higher lateral packing in the outer part of the SC for elderly. This can explain the decrease in TEWL
35 measured values rather than only SC thickening.
36
37
38

39 Both age groups showed similar water content at SC surface while elderly presented higher water
40 content in deep SC and viable epidermis.
41
42

43 Mechanical measurements showed a decrease in the elasticity and an increase in the fatigability with
44 age and were correlated with partially bound water. Highest correlation and anti-correlation values
45 were observed for the deepest part of the SC and the viable epidermis.
46
47
48

49 **Key words:** skin aging, *in vivo* Raman spectroscopy, biophysics parameters.
50
51
52
53

54 **Introduction**
55

56 Skin aging is a multifactorial phenomenon, a complex process that involves alterations at the
57 molecular, cellular, and tissue levels [1, 2]. There are two types of skin aging: intrinsic and extrinsic
58 aging (photo-aging) [3].
59
60

1
2
3 Chronological (intrinsic) aging affects the skin in a manner similar to other organs [4], it is related to
4 natural biological aging processes in sun-protected skin. Intrinsically aged skin appears smooth, pale,
5 and finely wrinkled [3]. Extrinsic aging is related to environmental, mainly UV-induced damage of the
6 epithelial (epidermis) and dermal connective tissues of the skin [1, 3, 4]. Photo-aged skin is coarsely
7 wrinkled and frequently characterized by abnormal pigmentation and telangiectasias [1, 3, 4].
8
9

10
11
12 Both processes intrinsic and extrinsic have overlapping biological, biochemical, and molecular
13 mechanisms [3, 4]. In the dermis, aging involves : *i.* degradation of several extracellular matrix proteins,
14 including collagen and elastic fibres [2, 3, 5], and *ii.* changes in the hydration state [2, 5]. Chronological
15 aging alters the collagen of the papillary dermis [5], reduces the hydration and compactness of collagen
16 fibres [2, 5], while photoaging causes a decrease in collagen stability by reducing collagen type VII
17 containing anchoring fibrils that contribute to the stabilization of the epidermal-dermal junction [4]
18 and altering proline and hydroxyproline residues in the reticular dermis [5]. Besides macroscopic signs
19 of aging, the degradation of the collagen and elastic fibre network induces a loss of elasticity and an
20 increase in the fatigability of the skin [6-8].
21
22

23
24
25 Aging induces also epidermal changes, which involve thinning of stratum spinosum and flattening of
26 the dermo-epidermal junction [9]. Senescent keratinocytes become resistant to apoptosis and may
27 survive longer increasing the risk of DNA and protein damage. The numbers of melanocytes decrease
28 and dysregulation of melanocyte density results in freckles, guttate hypo-melanosis, lentiginos and
29 nevi. The number of dendritic Langerhans cells also diminishes [9].
30
31

32
33
34 As elegantly explained by Tagami [10], despite the general decline of various bodily functions in
35 advanced age, the barrier function of the SC does not deteriorate but rather improves with aging. He
36 synthesized different studies reporting lower percutaneous absorption of topically applied substances
37 in aged skin [10]. Although the relative amount of intercellular lipids decreased [10-13], the trans
38 epidermal water loss (TEWL) did not increase [10, 12, 13].
39
40

41
42
43 Using confocal Raman spectroscopy, Boireau et al [11, 12, 14] and Choe et al [13] followed SC aging on
44 the forearm. Age ranges were 18-70 years for the former and 23-62 for the latter. Both studies
45 reported thickening of the SC with age [11-13] reflecting the reduced epidermal proliferation
46 associated with slower desquamation of the SC [10]. While both described a decrease in the lipid
47 content, only Choe et al. observed higher ordered organization [13].
48
49

50
51
52 SC hydration was also monitored but contradictory results were reported; Boireau et al [11] concluded
53 in a decrease in water content on exposed arm sites and no modifications in the normalized
54 concentration profiles of the different water mobility states. In opposite to that, Choe et al [13]
55 observed more hydrogen bound water molecules at the depth 10–30% of the SC thickness correlated
56
57
58
59
60

1
2
3 with the NMF profiles and lipid organizational order. The mismatch of these results was explained by
4 Choe et al. [13] by different data processing on some observations and the difference in age ranges on
5 others.
6
7
8
9

10
11 The present work is a part of a more global study interested in multiparametric characterization of
12 aging of the skin barrier. The first part of this study was focused on the evolution of skin surface lipids
13 (SSLs) content and composition with aging [15]. It showed a lower sebum content, together with
14 modification of the relative SSLs composition involving a significant reduction in the intensity of the
15 majority of lipid components in the hydrolipidic film, namely: glycerides (tri- and di-), free fatty acids,
16 waxes, cholesterol esters and squalene. Cholesterol content non significantly diminished while
17 monoglycerides, hydroxy-oxidosqualene (non-significantly) and 2,3-oxidosqualene (significantly)
18 increased with an inverse relationship between triglycerides and their hydrolytic products [15].
19
20
21
22
23
24

25 In this second part of the study, multiparametric biometric measurements together with *in vivo*
26 confocal Raman microspectroscopy were used for the characterization of skin barrier aging on the
27 forehead.
28
29
30
31
32
33
34
35
36
37
38
39
40
41
42
43
44
45
46
47
48
49
50
51
52
53
54
55
56
57
58
59
60

Materials and methods

Volunteers

This study was performed in agreement with the Helsinki Declaration. A written informed consent was established for each volunteer. 2 groups of healthy Caucasian women were enrolled: 22 young volunteers aged between 18 and 24 years (mean $21,8 \pm 0.35$); 18 old volunteers aged between 70 and 75 years (mean $72,1 \pm 0.38$). All subjects were non-smoking, presented Fitzpatrick's skin types between I and III, and a Body Mass Index (BMI) less than 27. No skin care products were applied to the measured sites and these sites were not washed with soaps or surfactants for at least 24 h prior the study. After an acclimation time of 20 min in an environmental controlled room ($22.6 \pm 0.3^{\circ}\text{C}$, $43 \pm 1\% \text{RH}$), the different physiological parameters were measured on the forehead. For Raman analyses, measurements were performed on 18 selected volunteers, 10 young aged between 18 and 24 years and 8 aged between 70 and 75 years. All volunteers completed the study.

Biometric measurements.

The measured values were Trans-Epidermal Water Loss (TEWL) using Tewameter TM300, the sebum content on the skin surface using Sebumeter SM815, and the elasticity parameters using Cutometer MPA580, all from (Courage+Khazaka electronic GmbH, Köln, Germany). The time/strain mode of the cutometer was used with 3 consecutive cycles of a 5-s suction application followed by a 3-s relaxation period. We used a 2mm diameter measuring probe and we applied a constant suction of 450mbarTo minimize the intra-individual variation, the presented biometric values are the mean of 3 measurements.

To evaluate colorimetric parameters and porphyrin levels, full face 2D images were captured by Visia-CR® imaging system (Canfield Scientific, New Jersey, USA), with different light modalities (cross-polarized light, parallel polarized light, UV). Colorimetric parameters were obtained with Colorskin® (Newtone Technologies, Lyon, France) software on the forehead and on the cheek: luminosity (L^*), red/green chromatic component (a^*), yellow/blue chromatic component (b^*), saturation (C^*), tint angle (h^*) and skin pigmentation (ITA). Porphyrin content was determined on the forehead and on the cheek, using home-made data processing. Two parameters were determined, *i.e.* area (obtained from the number of pixels) and volume (obtained from the integration of pixels intensities).

In vivo Raman spectroscopy

In vivo Raman investigations were performed using an *in vivo* confocal Raman optical microprobe (Horiba Scientific, Villeneuve d'Ascq, France) attached to a home-made movable arm allowing to easily position the probe on skin surface.

The set-up consists of a 660nm laser diode as excitation source; a probe-head including interferential and edge band pass filters for filtering incident laser line and Rayleigh scattering respectively; a long focal microscope objective MPLAN FLN 100X/NA 0.75 (Olympus, Japan) for focusing the excitation beam and capturing the scattered light (3 μm in-depth resolution).

The objective was coupled to a piezoelectric system, a 5 μm diameter fiber optic with coaxial two-fiber probe, one for excitation and the other for collection. Raman spectral in-depth profiles were collected from -6 μm of the skin surface to +30 μm with a 3 μm step.

Collected scattered light was analysed with a LabRAM HR Evolution (Horiba Scientific, Villeneuve d'Ascq, France) spectrograph by means of a high sensitivity CCD detector (Synapse) cooled to -70°C by Peltier effect and gratings of 300gr/mm permitting to achieve 4 cm^{-1} spectral resolution. Two spectral regions were investigated: the fingerprint region (400-1800 cm^{-1}) and the high wavenumbers (2600-3800 cm^{-1}). For each scan, a 2 seconds exposure time was used with 2 accumulations per spectrum. Each in-depth profile included 13 spectra for a total of 30 seconds acquisition time per profile.

Raman data analyses

The different data preprocessing and processing were performed using in house developed software under Matlab® environment (Mathworks, Natick, MA, USA). All spectra were corrected using Savitzky-Golay function on 11 points and baseline corrected using an automatic polynomial algorithm.

Curve fitting was carried out using the Least Squares Fitting algorithm. The algorithm allows to identify, by using second derivative, the number of sub-bands within a spectral region. It then automatically adjusts the combination of bands to best fit the spectral profile. The maximum shift of the sub-band position was set to $\pm 10 \text{ cm}^{-1}$, the bandwidth was fixed to 100 cm^{-1} , while intensity was left free to adapt to the fit. The quality of the fit was estimated by the standard error and the χ^2 values [16, 17].

Stratum corneum (SC) thickness

The SC surface was automatically detected based on the integrated intensity of the CH stretching band. The starting point is located at half of the intensity maximum reached at the end of the first regime (air) [18-20]. In depth scales were shifted to set the zero position at the starting point.

1
2
3 The boundary between the SC and viable epidermis was determined from water profiles as described
4 by Egawa *et al.* and Crowther *et al.* [13, 21-25]. The SC thickness is thus determined by calculating the
5 difference between the SC-viable epidermis boundary and the zero position.
6
7

8
9 For the comparison between young and elderly spectral profiles, the boundary between SC and viable
10 epidermis was normalized to 100% and depths were expressed in percentage of SC thickness.
11

12 *Lipids to Proteins evolution*

13
14
15 To follow the relative evolution of the lipid related spectral signatures compared to keratin related
16 features we have used the ratio of the CH₂ stretching bands (associated to lipids [26, 27]) to the CH₃
17 stretching bands (associated with proteins [16, 17]). This spectral parameter is described in the
18 literature [12, 13, 25, 28-30].
19
20
21

22 *Lipids compactness*

23
24
25 The lipids lateral packing was evaluated using the asymmetric to symmetric CH₂ stretching spectral
26 features ($v_{\text{asym}} \text{CH}_2 / v_{\text{sym}} \text{CH}_2$) (2850 cm⁻¹/2885 cm⁻¹). This ratio is generally used as an indicator of the
27 conformational state and lateral packing. High values are associated with higher trans content and a
28 compact organization while a decrease is indicative of a loosening [17, 27, 31-34].
29
30
31

32 *Water content and mobility*

33
34 To follow the water content within the SC, we used the bands ratio of OH stretching (3100-3800 cm⁻¹)
35 to CH stretching (2800-3000 cm⁻¹) [13, 16, 25, 35].
36
37

38
39 Spectral features associated with different types of water were assessed by band deconvolution. The
40 sub-bands decomposition proposed by Vyumvuhore *et al.* [16, 17] was applied in the present work,
41 *i.e.* tightly bound water centred at 3210 cm⁻¹, partially bound water at 3280 cm⁻¹ and 3345 cm⁻¹ and
42 unbound water at 3470 cm⁻¹ [16, 17].
43
44

45
46 The first sub-band is related to primary bound water which is tightly bound to the SC polar sites of
47 proteins and polar heads of lipids, constituting a first monolayer of water. Partially bound water is
48 bound to the first monolayer and to other SC molecular components This means that water molecules
49 interact partially with neighbouring molecules using only 2 or 3 of the 4 possible hydrogen bonds. The
50 evolution of the global partially bound water content was observed by plotting the sum of both sub-
51 bands. Unbound water is considered as water that is not directly linked to the SC components, thus
52 presenting no hydrogen bonds with SC lipids or proteins [16, 17, 34].
53
54
55
56
57
58
59
60

1
2
3 The OH stretching band deconvolution was also described by Sun *et al.* [36, 37] and adapted by Choe
4 et al. [13, 25] for SC water mobility. Deconvoluted bands from both methods lead to similar evolution
5 (see results section).
6
7

8 *Proteins folding*

9
10 The maximum position of $\nu_{\text{asym}}\text{CH}_3$ at $\sim 2930\text{ cm}^{-1}$, is related to the folding/unfolding process of proteins.
11 Folding of the proteins can be highlighted by a shift towards lower wavenumbers [13, 16, 17, 31, 34,
12 38].
13
14
15

16 *Statistical analysis*

17
18
19 Statistical analyses were performed using Matlab® environment (Mathworks, Natick, MA, USA). To
20 compare the spectral and biometric parameters within each group, a Shapiro-Wilk test for normality
21 was applied followed by the ANOVA test was used. Two-way analysis of variance for variation inter-,
22 and intra-groups for all the skin parameters has been presented as mean \pm Standard Deviation.
23 Variables that failed the Shapiro-Wilk normality test where compared with the non-parametric
24 Kruskal-Wallis test (*KW*).
25
26
27
28
29
30

31 Significance limits were set to P-values at 1% and 5%. P-values lower than 10% were used as tendency
32 indicators.
33
34

35
36 Pearson's correlation coefficient (*r*) calculation was employed to evaluate the linear relation between
37 Raman spectral markers and the measured physiological and biometric parameters, where the value *r*
38 = 1 means a perfect correlation while values higher than 0.5 are considered to describe correlate.
39
40
41
42
43
44
45
46
47
48
49
50
51
52
53
54
55
56
57
58
59
60

Results and discussion

Evolution of colorimetric parameters with age

Table 1 details the spectrometric parameters obtained with Visia-CR. No significant differences were obtained between both groups for forehead while highly significant discrimination can be observed for the cheek.

Colorimetric measurements: forehead				
Parameters	Young	Elderly	pValue	Age related modifications
L*	63.20 (± 0.77)	61.95 (± 1.07)	0.22	NS (KW)
a*	10.27 (± 0.44)	10.18 (± 0.64)	0.98	NS (KW)
b*	17.29 (± 0.83)	17.83 (± 0.78)	0.64	NS (KW)
C*	20.22 (± 0.83)	20.63 (± 0.89)	0.68	NS (KW)
h*	58.83 (± 1.30)	60.35 (± 1.42)	0.62	NS (KW)
ITA	37.763 (± 2.73)	33.63 (± 0.86)	0.18	NS (KW)
Colorimetric measurements: cheek				
Parameters	Young	Elderly	pValue	Age related modifications
L*	66.00 (± 0.59)	61.49 (± 1.03)	< 0.001	↘ (KW)
a*	11.94 (± 0.71)	14.76 (± 0.95)	0.02	↗ (anova)
b*	15.29 (± 0.62)	19.15 (± 0.75)	< 0.001	↗ (KW)
C*	19.62 (± 0.70)	24.32 (± 1.04)	< 0.001	↗ (KW)
h*	52.19 (± 1.82)	52.78 (± 1.48)	0.96	NS (KW)
ITA	46.30 (± 1.92)	30.94 (± 3.03)	< 0.001	↘ (KW)

Table 1: colorimetric parameters collected on the forehead and the cheek of young and elderly volunteers.

The opposite observations from both forehead and cheek may be related to a long-term protective role of the skin surface lipids present on the forehead. A similar observation on the role of Sebum lipids as protective barrier was described by Tagami [10]. In his review, he reported that sebum excretion and non-apparent sweating participate to the protection of the facial skin[10].

Variations of porphyrin related values with age

		Young	Elderly	pValue	Age related modifications
Cheek	Area	0.05 (± 0.007)	0.02 (± 0.003)	<0.001	↘
	Volume	3.95 (± 0.76)	1.01 (± 0.25)	<0.001	↘
Forehead	Area	0.044 (± 0.01)	0.013 (± 0.005)	0.007	↘
	Volume	3.52 (± 1.06)	0.89 (± 0.41)	0.03	↘

Table 2: Porphyrins values obtained with visia-CR

Secreted by bacteria in the pilosebaceous follicles, porphyrins are endogenous fluorophores which may participate to the absorbing and reflecting process of the light [39]. In addition, a correlation between sebaceous gland activity and presence of porphyrins in the frontal region has been demonstrated [40]. The decrease of porphyrin may be related to the decrease in the sebum content on the skin surface observed with skin aging (Fig. 02.A).

Evolution of mechanical parameters,

Parameters	Young	Elderly	pValue	Age related modifications
R1	0.11 (± 0.004)	0.15 (± 0.01)	0.002 (anova)	↗
R2	0.60 (± 0.02)	0.51 (± 0.02)	0.003 (KW)	↘
R4	0.16 (± 0.007)	0.21 (± 0.01)	<0.001 (anova)	↗
R5	0.61 (± 0.03)	0.44 (± 0.03)	<0.001 (KW)	↘
R7	0.33 (± 0.01)	0.22 (± 0.01)	<0.001 (KW)	↘
Q1	0.47 (± 0.02)	0.36 (± 0.02)	<0.001 (KW)	↘

Table 3: Mechanicals parameters obtained with Cutometer on volunteers forehead.

Table 3 shows the mean values of elasticity and fatigability parameters for young and elderly. Fatigability parameters (R1 and R4) increased with age while elasticity parameters (R2, R5, R7) and visco-elastic recovery (Q1) decreased.

In addition to Anova, Pearson's correlation coefficient (r) was calculated to evaluate the linear relation between mechanical markers and age (data not shown). Similar tendency was obtained with moderate correlation values ($\sim |0.55|$). R7 showed the higher anti-correlation coefficient ($r^2: -0.74$). This is in concordance with results obtained by Eklouh-Molinier *et al.* [6] who observed an increase in fatigability and a decrease of elasticity.

1
2
3 In addition to chemical protective barrier, skin provides mechanical protection against physical
4 stressors. With aging, the degradation of the collagen and elastic fibre network induces a loss of
5 elasticity and an increase in the fatigability of the skin [6-8].
6
7

8
9 Eklouh-Molinier *et al.* [6] applied partially least squares regression to highlight spectral features that
10 fits the best with mechanical properties associated with aging. CH₃ stretching as well as νC=O were
11 identified as markers for mechanical stress. Meanwhile, the correlation coefficients obtained were
12 around 0.2 and not enough to statically consider these spectral features for directly conduct
13 conclusions on the mechanical behaviour in a such complex system as the skin associated to a complex
14 phenomenon as the skin aging.
15
16
17
18

19
20 Even if the mechanical behaviour relies mainly on elastin and collagen fibres in the dermis, it has been
21 demonstrated that the SC presents a significant contribution in the overall mechanical properties of
22 the skin [6, 8]. In their study, Sano et al. [41] reported significant reduction of the elasticity of the
23 stratum corneum after repetitive UV_B exposure. The exposure concomitantly induced the formation
24 of wrinkles. This relationship suggests that reductions in elasticity of the stratum corneum are probably
25 one of the major factors in wrinkle formation. In a previous study, we have investigated the molecular
26 modifications due to the extension of SC by using Raman spectroscopy [38]. When SC was stretched,
27 alpha helix form of proteins unravelled and were converted into beta-sheet forms. In parallel, lipids in
28 *gauche* conformational order, which corresponds to less ordered lipid matrix, increases with strain.
29
30
31
32
33
34

35
36 Despite the high values of the correlation coefficient obtained in this study, it does not take into
37 account the complexity of the *in vivo* system.
38

39
40 At this stage of knowledge, correlation between vibrational features and mechanical parameters
41 should be considered as complementary information for the understanding of a complex phenomenon
42 and not to substitute one by another by trying to predict elasticity or fatigability from Raman spectra.
43
44
45
46
47
48
49
50
51
52
53
54
55
56
57
58
59
60

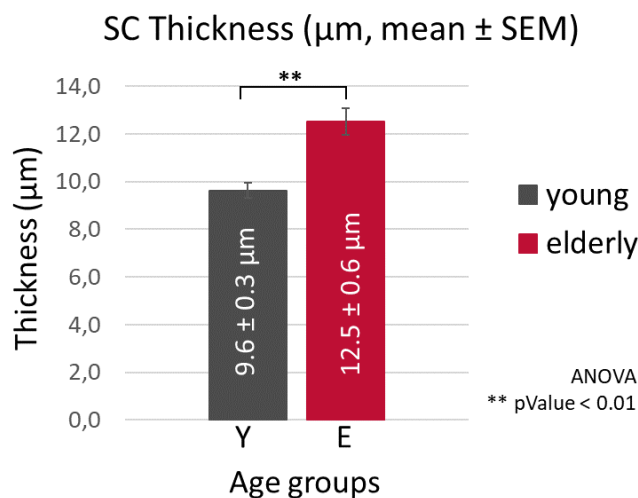
Increase of SC thickness with age

Figure 01: average thickness of SC (forehead) for both age groups.

The average of the Stratum Corneum thickness of forehead skin was determined to be $9.6 \pm 0.3\mu\text{m}$ for young volunteers and $12.5 \pm 0.6 \mu\text{m}$ for elderly (figure 01). The SC of elderly is significantly thicker than the SC of younger ($p < 0.01$, ANOVA).

These results are in concordance with results reported by Egawa *et al* [21], Boireau-Adamezyk *et al.* [12] and Choe *et al.* [13]

Despite the fact that overall skin becomes thinner with age [10], the thickness of the SC increased. This can be explained by reduced epidermal proliferation associated with slower desquamation of the SC, higher intercorneal cohesiveness [10] and increased corneocytes size in aged SC compared to young [10, 42, 43].

Decrease of surface lipids and SC lipids content with age

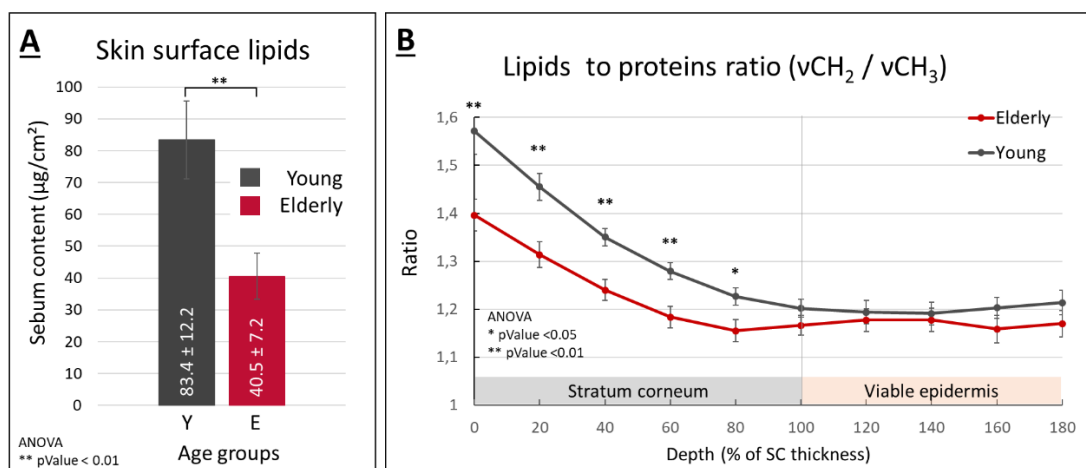


Figure 02: A. Sebum content on skin surface, B. Lipids to keratin ratio from to SC surface to the viable epidermis.

At skin surface, our results showed a significant decrease of the amount of sebum for elderly ($40.5 \pm 7.2 \mu\text{g}/\text{cm}^2$) compared to young volunteers ($83.4 \pm 12.2 \mu\text{g}/\text{cm}^2$) (figure 02.A). This corresponds to the significant reduction of the majority of lipid components in the hydrolipidic film observed with HT-GC/MS in the first part of this study [15].

In parallel, in-depth *in vivo* Raman profiles highlighted a significant decrease of lipids to proteins ratio overall the thickness of the SC (figure 02.B). Similar significant reduction was reported by Boireau-Adamezyk et al. [12, 14] while Choe et al [13] indicated a non-significant decrease in lipids against NMF. An explanation may be the age range of the volunteers enrolled in their study.

It is worthy to notice that the differences in the relative amounts between young and aged groups increased gradually from depth (SC/viable epidermis interface) to the SC surface.

The lower ratio values and the in-depth gradient may be explained, on one hand, by reduced intercellular lipid production in the SC [10] and in skin surface lipids (SSLs) [15] and on the other hand, by the presence of a lower number but larger corneocytes covering the aged skin [10]. This was also used to explain the higher relative amount of amino acids with age measured by Takahashi et al. [44].

The increase of keratin content was also reported by Kambayashi., et al. [45] on effects of chronic low-dose UV irradiation. They postulated that this increase may be involved in the alteration of the physical properties of the skin and wrinkles formation.

Decrease of trans epidermal water loss and increase of lipids compactness at SC surface with age

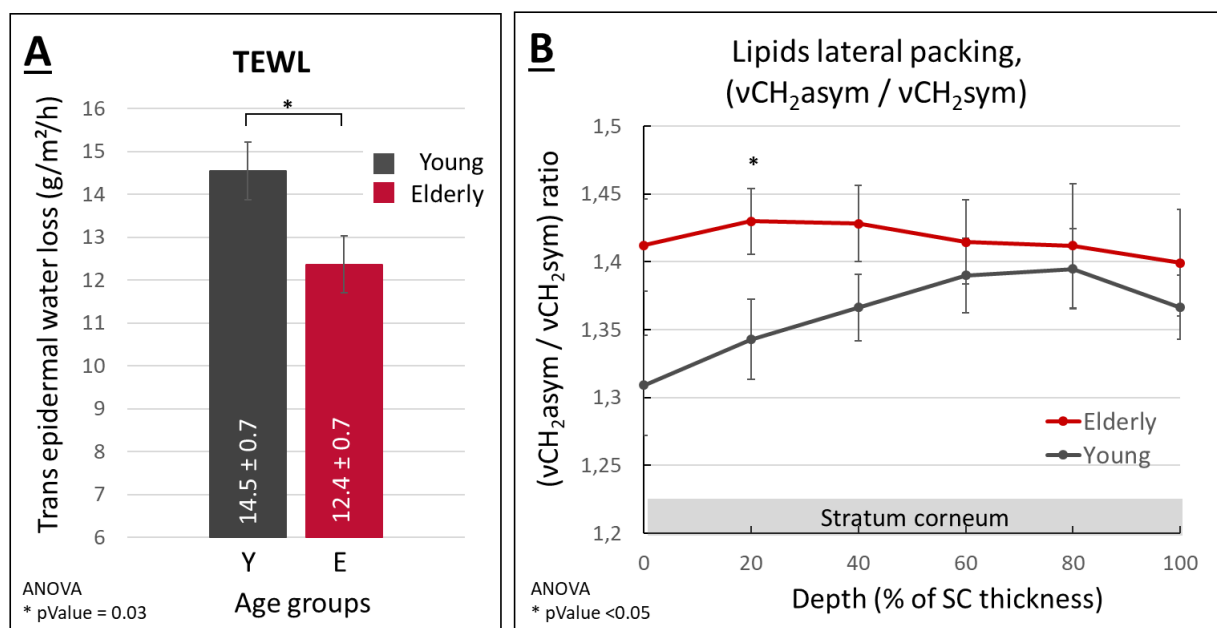


Figure 03: A. Trans epidermal water loss (TEWL), B. Lateral packing of lipids in the SC.

Trans Epidermal Water Loss diminished significantly for elderly (figure 03.A). This reduction in the water loss is largely reported in the literature [12, 46-49].

As the water loss is directly related to the barrier function of the SC, lipids lateral packing was followed based on CH₂ asymmetric to CH₂ symmetric stretching.

Two observations can be made from the profiles in figure 03.B. Firstly, for young volunteers, we observed a gradual decrease in the lateral packing moving from depth to the surface. Elderly SC showed no in-depth related gradual decrease leading to the second observation, *i.e.*, a higher lateral packing in the outer part of the SC with significant difference at around 20 % depth.

The first observation is in concordance with observations of Boireau-Adamezyk et al. [12]. A possible explanation may be the relation between the organizational order of lipids and the desquamation process. This latter is complex molecular and enzymatic phenomenon that impacts keratin, corneodesmosomes, lipids and the other components in the SC [10].

The second observation is contradictory with a previous study of our group [32] which reported a loosening in the lipid matrix. In this previous study, the instrumental set-up did not include microspectroscopic measurements and data were collected with a fibre probe giving around 100 μm in depth collection for each spectrum. The low spatial resolution didn't allow to directly observe

1
2
3 spectral features related to lipids. In order to reach this information, lipids were extracted from SC and
4 their *in vivo* signature was obtained from difference spectra obtained on skin surface before and after
5 lipids extraction.
6
7

8
9 Boireau et al [12] reported no significant difference in lipid compactness between both age groups
10 while Choe et al. [13] results mentioned an increase in the lateral packing and conformational order
11 with age. Results in total agreement with the in-depth profiles plotted in figure 03.B. In addition to
12 that, the significant differences were observed by Choe et al. [13] between 10 and 30 % of the SC
13 thickness which is concordant with the significant increase observed at 20% in our results.
14
15
16

17
18 The enhancement of the barrier function in aged skin was also described by Tagami [10]. As mentioned
19 by Choe et al. [13, 50], this can explain the decrease in TEWL measured values rather than only SC
20 thickening.
21
22

23
24 Meanwhile, it is important to keep in mind the complexity of the skin aging and to consider the
25 observations as inter-correlated and not as separate observations; e.g. the observed absence of
26 gradual decrease in lipids organisation towards surface in elderly SC cannot be dissociated from the SC
27 thickening without being able at this stage to describe a cause to effect relationship.
28
29
30
31
32
33
34
35
36
37
38
39
40
41
42
43
44
45
46
47
48
49
50
51
52
53
54
55
56
57
58
59
60

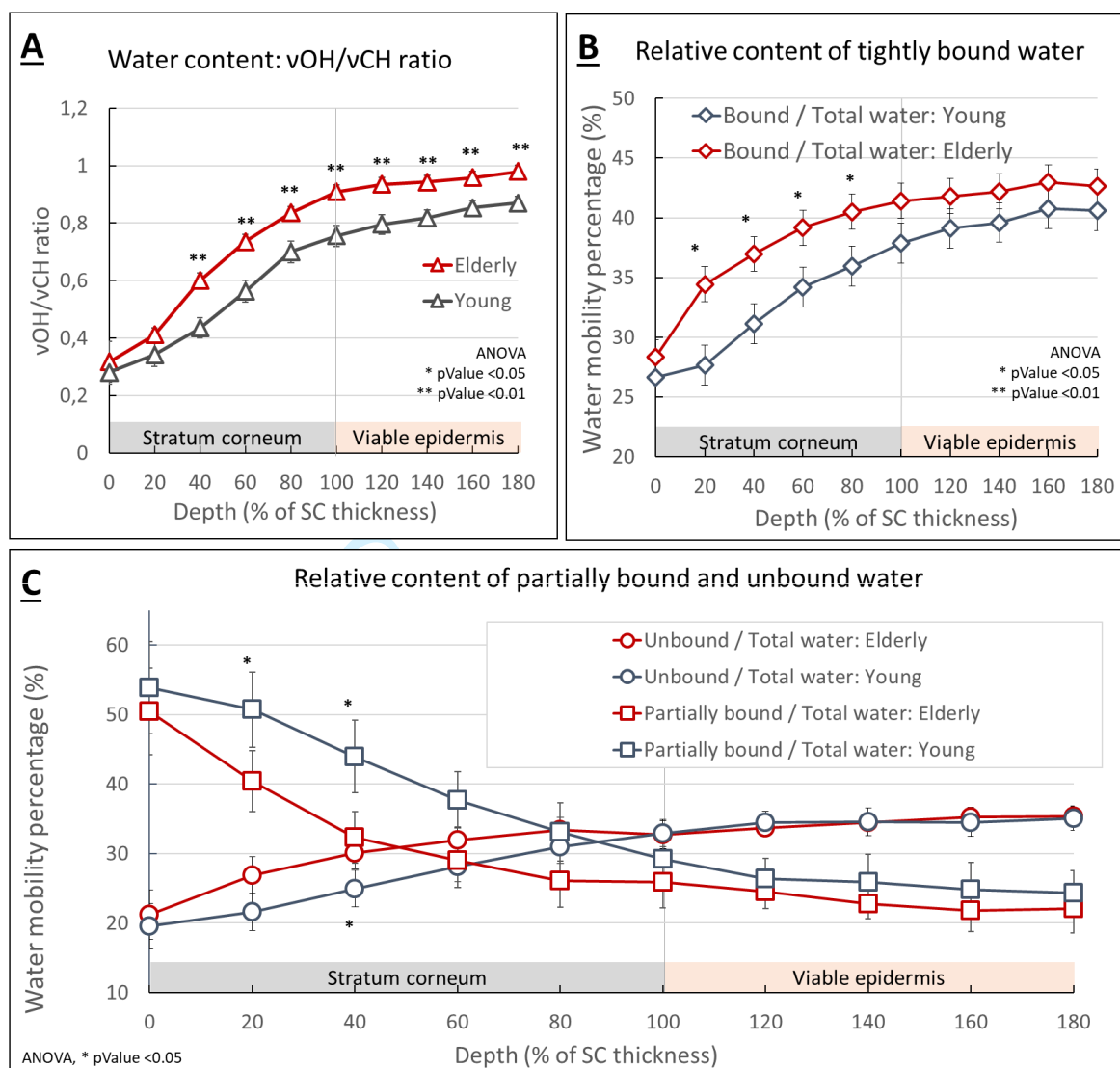
Evolution of water gradients with age

Figure 04: A. water content in SC and viable epidermis (vOH / vCH ratio). B. percentage of tightly bound water. C. percentages of partially bound and unbound water.

Similar water content at SC surface for both age groups and higher water content for elderly in deep SC and viable epidermis:

The analysis of the vOH/vCH ratio (figure 04.A) presented the classical evolution with an increase from surface to reach a plateau after the SC/viable epidermis interface. Comparison between both age groups showed no difference at the surface of the SC, non-significant increase at 10% depth followed by significantly higher water content down to SC/viable epidermis interface and in the viable epidermis.

1
2
3 Using ATR-FTIR; Machado et al. [42] found no evident difference in water content at the skin surface
4 (in contact with ATR crystal) between age groups. This is in perfect agreement with the plot in figure
5 04.A at the surface of the SC.
6
7

8
9 The higher amount of water in the loose skin tissue and deeper parts of the SC was already pointed by
10 Kligman [46] and Tagami [10].
11
12
13
14

15 *Increase in the tightly bound water relative amounts with age:*
16

17
18 In figure 04.B, we plotted the normalised tightly bound to total water content. While the observed
19 gradual decrease for both young and elderly was in agreement with Boireau et al. observations [12],
20 the comparison between age groups are not concordant. In fact, results presented in figure 04.B show
21 a significant increase of the tightly bound water with age. Similar observations were reported by Choe
22 et al. [13]. For their study, they have used a different method for bands selection. In their classification,
23 the DDAA-OH water related band was around 3226 cm^{-1} , very close to our tightly bound water band at
24 3210 cm^{-1} .
25
26
27
28
29

30 The lower significance reported in their study can be explained by the reduced age range enrolled in
31 their study and the lower number of volunteers for the statistical validation. The observation of higher
32 amounts of NMF was given as an explanation for the increase of this type of water [13].
33
34
35
36
37

38 *Lower percentage of partially bound water and higher percentage of unbound water within*
39 *elderly SC:*
40
41

42 Finally, in figure 04.C, the plotted profiles represent the percentage of partially bound and unbound
43 water in the SC and the viable epidermis. As for figure 04.B, the type-related water gradient from depth
44 to surface is in agreement with Boireau-Adamezyk et al. [12, 14], but not the comparison between age
45 groups [11].
46
47
48

49 The relative amounts of partially bound water decrease when moving from surface to reach a plateau
50 for the viable epidermis. Lower values in the percentage of partially bound water are observed in the
51 SC (20% down to 100%) while the percentage is not significantly different for viable epidermis. In Choe
52 et al. study [13], the DA-OH related band at 3342 cm^{-1} is close to one of our two defined partially bound
53 water bands (3280 cm^{-1} and 3345 cm^{-1}). The separate observation of each of these two bands followed
54 the same tendency with lower significance. The sum is thus used.
55
56
57
58
59
60

1
2
3 In contrast to the evolution of partially bound water, the unbound water fractions increase going from
4 the surface of the SC to reach a plateau for the viable epidermis. The relative amounts of unbound
5 water present non-significantly higher levels for elderly in the SC (significant at 40% of SC thickness).
6
7 The levels are equivalent for viable epidermis. A possible explanation of the higher amounts was
8 advanced by Choe et al. in their work on the forearm [13] and related this increase to the enhancement
9 to the lipids organisational order near to the SC surface. This is concordant with the dynamic of the
10 unbound water through the SC.
11
12
13
14

15 From the observations in figure 04.B and 04.C, tightly bound and unbound water increased with age
16 as well as the total water content. Meanwhile, it was widely advanced that with aging, skin becomes
17 thinner, dry and rough [10, 51]. The sensation of dry skin is frequently related to tightening and
18 mechanical stress. This may be associated to a reduction of the partially bound water within the SC.
19
20
21
22
23
24

25 *Balance between partially bound and unbound water: shallower position of equilibrium depth*
26 *for elderly*
27
28

29 In addition to the up-mentioned observations, it is worthy to notice that the intersection between both
30 partially bound and unbound lines for both aged and young epidermis. The intersection marks the
31 balance between both types of water. In young SC, the balance was observed around 90% of SC
32 thickness (figure 04.C). This means that partially bound water (bound to other molecular components
33 within the SC) was higher in almost all the SC. For elderly, the balance point was around 50 % of SC
34 thickness. To the far to our knowledge, this work is the first to highlight the depth of the balance point
35 and its variation along age.
36
37
38
39
40
41
42
43
44
45
46
47
48
49
50
51
52
53
54
55
56
57
58
59
60

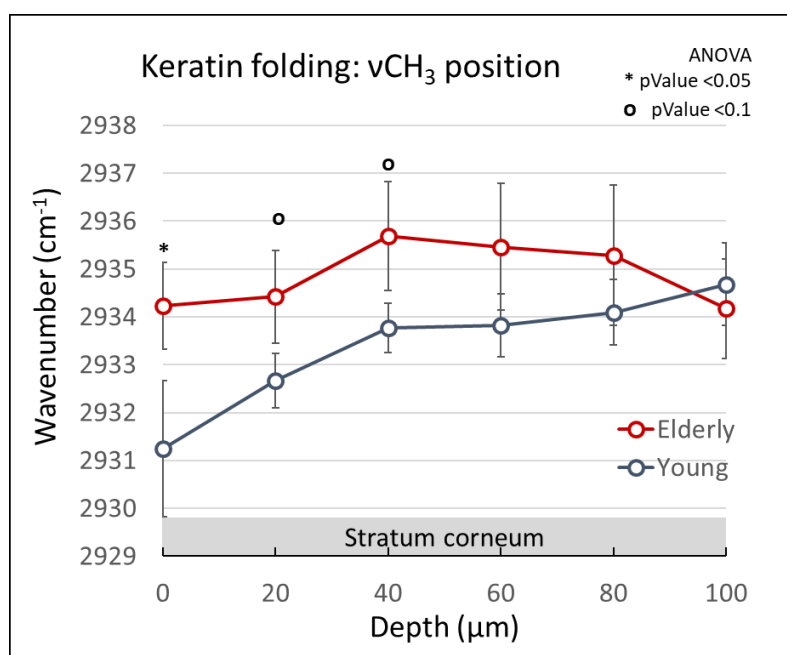
Effect of age on keratin folding

Figure 05: keratin folding observed by following the vCH₃ maximum position.

The folding status of the keratin, *i.e.* tertiary structure, was also monitored by following the position of the maximum of the $\nu_{\text{asym}}\text{CH}_3$ band around 2932 cm⁻¹ (figure 05). A shift of towards lower wavenumbers reveals folding of keratin thus favouring the intramolecular interactions [16, 17, 38].

The maximum position of this band is higher in aged SC revealing an unfolding of keratin (significant only at the surface) in concordance with Choe et al. [13] who reported no significant tendency.

The observed line of aged SC in figure 05 may be explained by connecting with other observations related to the lack of desquamation and the enhancement of the lipid barrier as well as the complex equilibrium between the three types of water.

Indeed, in our *in vitro* investigations [16, 17, 38] on SC samples, the variation of relative humidity led to variations in the unbound and partially bound water. The experimental set-up did not allow modifications in the tightly bound water. Thus, the evolution in the partially bound water were the only ones to correlate with the folding/unfolding of keratin and to the lateral packing of lipids.

In the present study, the water mobility showed modifications in the three types of water with age, particularly in tightly bound water. This leads to a more complex observations and does not mean that keratin fibres are not affected by water content as suggested by Choe et al. [13].

In addition to that, with age, the slower desquamation of the SC is also related to a deregulation in the enzymatic degradation of corneodesmosomes. Corneodesmosomes are the most important adhering junctions, providing strength for the SC structure made of corneocytes [52, 53]. This maintains higher intercorneal cohesiveness [10] and directly impacts the tertiary structure of keratin favouring the unfolding.

Correlation between mechanical parameters and in depth collected Raman descriptors.

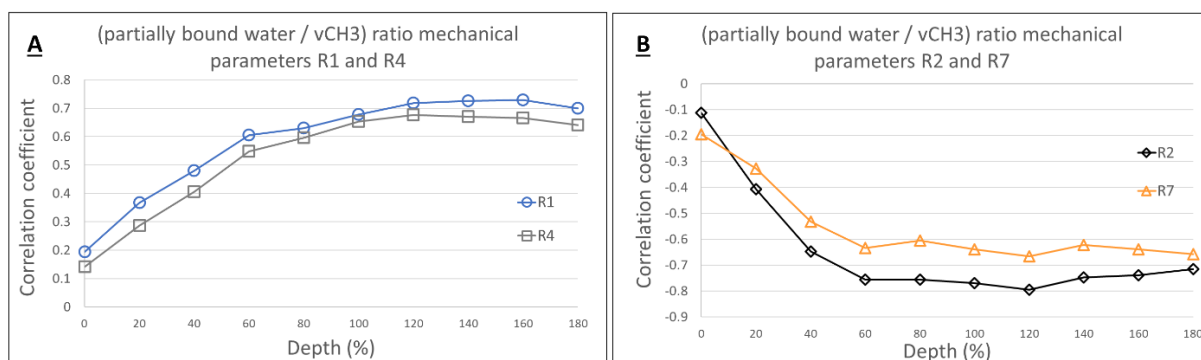


Figure 06: A, B. Correlation between partially bound water to CH_3 stretching ratio and mechanical parameters (A: R1 and R4, B: R2 and R7).

Pearson's correlation coefficients were calculated between the mechanical parameters obtained with the cutometer and the different Raman descriptors in function of depth. Highest correlation values were obtained with the ratio of partially bound water to CH_3 stretching (proteins) (figure 06.A and 06.B).

The correlations of fatigability parameters (R1 and R4) and the partially bound water to CH_3 stretching ratio is shown in figure 06.A. Very low correlation values can be observed at the surface of the SC and increased gradually when moving deeper to reach plateau between 80% and 100% of SC thickness. The correlations with elasticity parameters (R2 and R7) (figure 06.B) showed an anti-correlation that reached a plateau around 60% of SC thickness. Highest correlation and anti-correlation values are thus obtained for the deepest part of the SC and the viable epidermis.

These observations confirmed, on the one hand, the relation between partially bound water and mechanical stress. On the other hand, they related the fatigability and the elasticity parameters measured by the cutometer to the deepest parts of SC and viable epidermis.

Conclusion

The present work gathered multiparametric measurements for the characterization of cutaneous aging and the possible adaptations in the skin of people over 70 years.

At skin surface, our results showed a significant decrease of the amount of sebum for elderly compared to young volunteers. This corresponds to the significant reduction of most lipid components in the hydrolipidic film observed with HT-GC/MS in the first part of this study [15]. In parallel, in-depth in vivo Raman profiles highlighted a significant decrease of lipids to proteins ratio overall the thickness of the SC.

In opposition to younger volunteers, where a gradual decrease in the lateral packing and a gradual folding of keratin fibers moving from depth to the surface were observed; Elderly SC didn't show an in-depth related gradual variation in lipids packing or keratin folding. These observations, as well as the thickening of the SC may be related to the slower desquamation process in aged skin.

Despite the decrease in the lipids amounts, higher lateral packing in the outer part of the SC was observed for elderly. This can explain the decrease in TEWL measured values rather than only SC thickening.

Both age groups showed similar water content at SC surface while elderly presented higher water content in deep SC and viable epidermis. This is related to an increase in the tightly bound and unbound water relative amounts with age. Meanwhile, lower percentage of partially bound water were observed.

The intersection between unbound and partially bound water lines marks the balance between both types of water. The balance point was observed around 90% of SC thickness for young volunteers and around 50 % of SC thickness for elderly.

The sensation of dry skin with age is frequently related to tightening and mechanical stress. This may be associated to a reduction of the partially bound water within the SC. This is concordant with the decrease in the elasticity and the increase in the fatigability with age and the high correlations obtained between mechanical parameters and partially bound water.

Finally, it is important to notice that the highest correlation and anti-correlation values were obtained for the deepest part of the SC and the viable epidermis.

References

1. Peysselon, F. and S. Ricard-Blum, *Understanding the biology of aging with interaction networks*. Maturitas, 2011. **69**(2): p. 126-130.
2. Nguyen, T.T., et al., *Raman comparison of skin dermis of different ages: focus on spectral markers of collagen hydration*. Journal of Raman Spectroscopy, 2013. **44**(9): p. 1230-1237.
3. Gonzaga, E.R., *Role of UV Light in Photodamage, Skin Aging, and Skin Cancer*. American Journal of Clinical Dermatology, 2009. **10**(Supplement 1): p. 19-24.
4. Scharffetter-Kochanek, K., et al., *Photoaging of the skin from phenotype to mechanisms*. Experimental Gerontology, 2000. **35**(3): p. 307-316.
5. Villaret, A., et al., *Raman characterization of human skin aging*. Skin Research and Technology, 2018. **25**(3): p. 270-276.
6. Eklouh-Molinier, C., et al., *In vivo confocal Raman microspectroscopy of the human skin: highlighting of spectral markers associated to aging via a research of correlation between Raman and biometric mechanical measurements*. Anal Bioanal Chem, 2015. **407**(27): p. 8363-72.
7. Naylor, E.C., R.E.B. Watson, and M.J. Sherratt, *Molecular aspects of skin ageing*. Maturitas, 2011. **69**(3): p. 249-256.
8. Biniek, K., K. Levi, and R.H. Dauskardt, *Solar UV radiation reduces the barrier function of human skin*. Proc Natl Acad Sci U S A, 2012. **109**(42): p. 17111-6.
9. Wulf, H.C., et al., *Skin aging and natural photoprotection*. Micron, 2004. **35**(3): p. 185-191.
10. Tagami, H., *Functional characteristics of the stratum corneum in photoaged skin in comparison with those found in intrinsic aging*. Archives of Dermatological Research, 2007. **300**(S1): p. 1-6.
11. Boireau-Adamezyk, E., A. Baillet-Guffroy, and G.N. Stamatas, *Mobility of Water Molecules in the Stratum Corneum: Effects of Age and Chronic Exposure to the Environment*. Journal of Investigative Dermatology, 2014. **134**(7): p. 2046-2049.
12. Boireau-Adamezyk, E., A. Baillet-Guffroy, and G.N. Stamatas, *Age-dependent changes in stratum corneum barrier function*. Skin Res Technol, 2014. **20**(4): p. 409-15.
13. Choe, C., et al., *Age related depth profiles of human Stratum Corneum barrier-related molecular parameters by confocal Raman microscopy in vivo*. Mech Ageing Dev, 2017.
14. Boireau-Adamezyk, E., A. Baillet-Guffroy, and G.N. Stamatas, *The stratum corneum water content and natural moisturization factor composition evolve with age and depend on body site*. International Journal of Dermatology, 2021.
15. Rigal, A., et al., *Skin surface lipid composition in women: increased 2,3-oxidosqualene correlates with older age*. Eur J Dermatol, 2020.
16. Vyumvuhore, R., et al., *The relationship between water loss, mechanical stress, and molecular structure of human stratum corneum ex vivo*. J Biophotonics, 2015. **8**(3): p. 217-25.
17. Vyumvuhore, R., et al., *Effects of atmospheric relative humidity on Stratum Corneum structure at the molecular level: ex vivo Raman spectroscopy analysis*. Analyst, 2013. **138**(14): p. 4103-11.
18. Tfayli, A., O. Piot, and M. Manfait, *Confocal Raman microspectroscopy on excised human skin: uncertainties in depth profiling and mathematical correction applied to dermatological drug permeation*. J Biophotonics, 2008. **1**(2): p. 140-53.
19. Tfayli, A., et al., *Follow-up of drug permeation through excised human skin with confocal Raman microspectroscopy*. Eur Biophys J, 2007.
20. Caspers, P.J., et al., *In vivo confocal Raman microspectroscopy of the skin: noninvasive determination of molecular concentration profiles*. J Invest Dermatol, 2001. **116**(3): p. 434-42.

- 1
 - 2
 - 3
 - 4
 - 5
 - 6
 - 7
 - 8
 - 9
 - 10
 - 11
 - 12
 - 13
 - 14
 - 15
 - 16
 - 17
 - 18
 - 19
 - 20
 - 21
 - 22
 - 23
 - 24
 - 25
 - 26
 - 27
 - 28
 - 29
 - 30
 - 31
 - 32
 - 33
 - 34
 - 35
 - 36
 - 37
 - 38
 - 39
 - 40
 - 41
 - 42
 - 43
 - 44
 - 45
 - 46
 - 47
 - 48
 - 49
 - 50
 - 51
 - 52
 - 53
 - 54
 - 55
 - 56
 - 57
 - 58
 - 59
 - 60
21. Egawa, M., T. Hirao, and M. Takahashi, *In vivo estimation of stratum corneum thickness from water concentration profiles obtained with Raman spectroscopy*. *Acta Derm Venereol*, 2007. **87**(1): p. 4-8.
22. Bielfeldt, S., et al., *Assessment of human stratum corneum thickness and its barrier properties by in-vivo confocal Raman spectroscopy*. *International Journal of Cosmetic Science*, 2009. **31**(6): p. 479-480.
23. Crowther, J.M., et al., *Measuring the effects of topical moisturizers on changes in stratum corneum thickness, water gradients and hydration in vivo*. *Br J Dermatol*, 2008. **159**(3): p. 567-77.
24. Hancewicz, T.M., et al., *A Consensus Modeling Approach for the Determination of Stratum Corneum Thickness Using In-Vivo Confocal Raman Spectroscopy*. *Journal of Cosmetics, Dermatological Sciences and Applications*, 2012. **02**(04): p. 241-251.
25. Choe, C., J. Lademann, and M.E. Darvin, *Depth profiles of hydrogen bound water molecule types and their relation to lipid and protein interaction in the human stratum corneum in vivo*. *The Analyst*, 2016. **141**(22): p. 6329-6337.
26. Guillard, E., et al., *Thermal dependence of Raman descriptors of ceramides. Part II: effect of chains lengths and head group structures*. *Anal Bioanal Chem*, 2011. **399**(3): p. 1201-1213.
27. Tfayli, A., et al., *Thermal dependence of Raman descriptors of ceramides. Part I: effect of double bonds in hydrocarbon chains*. *Anal Bioanal Chem*, 2010. **397**(3): p. 1281-96.
28. Gniadecka, M., et al., *Structure of water, proteins, and lipids in intact human skin, hair, and nail*. *J Invest Dermatol*, 1998. **110**: p. 393-398.
29. Gniadecka, M., et al., *Water and protein structure in photoaged and chronically aged skin*. *J Invest Dermatol*, 1998. **111**(6): p. 1129-33.
30. Choe, C., J. Lademann, and M.E. Darvin, *Lipid organization and stratum corneum thickness determined in vivo in human skin analyzing lipid-keratin peak (2820-3030 cm⁻¹) using confocal Raman microscopy*. *Journal of Raman Spectroscopy*, 2016. **47**(11): p. 1327-1331.
31. Vyumvuhore, R., et al., *Vibrational spectroscopy coupled to classical least square analysis, a new approach for determination of skin moisturizing agents' mechanisms*. *Skin Res Technol*, 2014. **20**(3): p. 282-92.
32. Tfayli, A., et al., *Raman spectroscopy: feasibility of in vivo survey of stratum corneum lipids, effect of natural aging*. *European Journal of Dermatology*, 2012. **22**(1): p. 36-41.
33. Guillard, E., et al., *Thermal dependence of Raman descriptors of ceramides. Part I: effect of double bonds in hydrocarbon chains*. *Anal Bioanal Chem*. **Accepted**.
34. Quatela, A., et al., *In vivo Raman Microspectroscopy: Intra- and Intersubject Variability of Stratum Corneum Spectral Markers*. *Skin Pharmacol Physiol*, 2016. **29**(2): p. 102-9.
35. Biniek, K., et al., *Measurement of the Biomechanical Function and Structure of Ex Vivo Drying Skin Using Raman Spectral Analysis and its Modulation with Emollient Mixtures*. *Exp Dermatol*, 2018. **27**(8): p. 901-908.
36. Sun, Q., *The Raman OH stretching bands of liquid water*. *Vibrational Spectroscopy*, 2009. **51**(2): p. 213-217.
37. Sun, Q., *Local statistical interpretation for water structure*. *Chemical Physics Letters*, 2013. **568-569**: p. 90-94.
38. Vyumvuhore, R., et al., *Raman spectroscopy: a tool for biomechanical characterization of Stratum Corneum*. *Journal of Raman Spectroscopy*, 2013. **44**(8): p. 1077- 1083.
39. Sinichkin, Y.P., *In Vivo Fluorescence Spectroscopy of the Human Skin: Experiments and Models*. *Journal of Biomedical Optics*, 1998. **3**(2): p. 201.
40. Gabarra Almeida Leite, M. and P.M.B.G. Maia Campos, *Correlations between sebaceous glands activity and porphyrins in the oily skin and hair and immediate effects of dermocosmetic formulations*. *Journal of Cosmetic Dermatology*, 2020. **19**(11): p. 3100-3106.
41. Sano, T., et al., *The formation of wrinkles caused by transition of keratin intermediate filaments after repetitive UVB exposure*. *Archives of Dermatological Research*, 2004. **296**(8): p. 359-365.

- 1
- 2
- 3 42. Machado, M., J. Hadgraft, and M.E. Lane, *Assessment of the variation of skin barrier function*
4 *with anatomic site, age, gender and ethnicity*. International Journal of Cosmetic Science, 2010.
5 **32**(6): p. 397-409.
- 6 43. Plewig, G., *Regional Differences of Cell Sizes in the Human. Stratum Corneum Part II. Effects of*
7 *Sex and Age*. Journal of Investigative Dermatology, 1970. **54**(1): p. 19-23.
- 8 44. Takahashi, M. and T. Tezuka, *The content of free amino acids in the stratum corneum is*
9 *increased in senile xerosis*. Archives of Dermatological Research, 2004. **295**(10): p. 448-452.
- 10 45. Kambayashi, H., et al., *Involvement of changes in stratum corneum keratin in wrinkle formation*
11 *by chronic ultraviolet irradiation in hairless mice*. Experimental Dermatology, 2003. **12**: p. 22-
12 27.
- 13 46. Kligman, A.M., *Perspectives and Problems in Cutaneous Gerontology*. Journal of Investigative
14 Dermatology, 1979. **73**(1): p. 39-46.
- 15 47. Leveque, J.L., et al., *In Vivo Studies of the Evolution of Physical Properties of the Human Skin*
16 *with Age*. International Journal of Dermatology, 1984. **23**(5): p. 322-329.
- 17 48. Conti, A., M.E. Schiavi, and S. Seidenari, *Capacitance, transepidermal water loss and causal*
18 *level of sebum in healthy subjects in relation to site, sex and age*. International Journal of
19 Cosmetic Science, 1995. **17**(2): p. 77-85.
- 20 49. Wilhelm, K.P., *Skin aging. Effect on transepidermal water loss, stratum corneum hydration, skin*
21 *surface pH, and casual sebum content*. Archives of Dermatology, 1991. **127**(12): p. 1806-1809.
- 22 50. Choe, C., J. Lademann, and M.E. Darvin, *Gaussian-function-based deconvolution method to*
23 *determine the penetration ability of petrolatum oil into in vivo human skin using confocal*
24 *Raman microscopy*. Laser Physics, 2014. **24**(10).
- 25 51. El-Domyati, M., et al., *Intrinsic aging vs. photoaging: a comparative histopathological,*
26 *immunohistochemical, and ultrastructural study of skin*. Experimental Dermatology, 2002.
27 **11**(5): p. 398-405.
- 28 52. Levi, K., et al., *Effect of Corneodesmosome Degradation on the Intercellular Delamination of*
29 *Human Stratum Corneum*. Journal of Investigative Dermatology, 2008. **128**(9): p. 2345-2347.
- 30 53. Kitajima, Y., *Implications of normal and disordered remodeling dynamics of*
31 *corneodesmosomes in stratum corneum*. Dermatologica Sinica, 2015. **33**(2): p. 58-63.
- 32
- 33
- 34
- 35
- 36
- 37
- 38
- 39
- 40
- 41
- 42
- 43
- 44
- 45
- 46
- 47
- 48
- 49
- 50
- 51
- 52
- 53
- 54
- 55
- 56
- 57
- 58
- 59
- 60